American Mineralogist, Volume 74, pages 1317–1324, 1989

Chemistry of alkali-deficient schorls from two tourmaline-dumortierite deposits

FRANKLIN F. FOIT, JR.
Department of Geology, Washington State University, Pullman, Washington 99164, U.S.A.
YVES FUCHS
Ver 63, Université Pierre et Marie Curie, 4 Place Jussieu, 75005 Paris, France
PAUL E. MYERS
Department of Geology, University of Wisconsin, Eau Claire, Eau Claire, Wisconsin 54701, U.S.A.

ABSTRACT

Aluminous, alkali-deficient schorls occur with dumortierite in hydrothermally altered tuffs at Jack Creek, Jefferson County, Montana, and Ben Lomond, Hervey Range, North Queensland, Australia. The composition of tourmaline from both deposits, e.g., that of a schorl from Jack Creek,

$$(\square_{0.88}Na_{0.11}Ca_{0.01})(Al_{1.51}Fe^{2+}_{0.84}Fe^{3+}_{0.30}Mg_{0.14}\square_{0.20}Ti_{0.01})(Al_{5.46}Fe^{2+}_{0.54})(BO_3)_3(Si_{5.98}Al_{0.02})O_{18}(OH)_4,$$

closely approaches that of the alkali-defect end-member,

$$\square(R^{2+}_2R^{3+})Al_6(BO_3)_3Si_6O_{18}(OH)_4,$$

in response to the alkali-defect substitution, $R^{+} + R^{2+} = \square + R^{3+}$. In addition, tourmalines with a small alkali defect component frequently show significant $^{[4]}Al$ substitution, as shown by the composition of this crystal from the Jack Creek deposit,

$$(Na_{0.54}\square_{0.42}K_{0.04})(Al_{1.64}Fe^{2+}_{0.68}Fe^{3+}_{0.24}\square_{0.24}Mg_{0.19}Ti_{0.01})(Al_{5.57}Fe^{2+}_{0.43})(BO_3)_3(Si_{5.44}Al_{0.56})O_{18}(OH)_4.$$

In the schorls from Jack Creek, substitution of Al for Si in the six-membered ring is charge-balanced by substitution of Al for divalent cations in the octahedral sites (Tschermak's subsitution). In the schorls from the external zone of the Ben Lomond deposit, $^{[4]}Al$ substitution is primarily charge-compensated by either substitution of (Na,Ca) for a vacancy or Ca for Na in the 9-coordinated alkali-site. This accounts for the limited alkali-site defect found in Ben Lomond tourmalines, which have the most extensive $^{[4]}Al$ substitution. The coupling of tetrahedral- and alkali-site occupancies appears to help satisfy the charge-saturation requirements of the oxygen atoms shared by these sites.

The sensitivity of chemistry of tourmaline to the chemical and physical conditions that prevail during its crystallization emphasize its potential as a petrologic indicator mineral.

INTRODUCTION

Tourmaline has been recognized for its compositional variability since the late nineteenth century (Riggs, 1888; Penfield and Foote, 1899). This compositional variability, coupled with the difficulty of analyzing for B, delayed establishment of its formula and subsequent recognition of solid solution among its three earliest-recognized end-members, schorl, dravite, and elbaite. In succeeding decades, additional compositional variations and end-members were recognized; an excellent synopsis is given by Henry and Guidotti (1985). This ternary system is characterized by two complete solid-solution series, schorl-dravite and schorl-elbaite, with an apparent absence of solid solution of the type $2Mg^{2+} = Li^{+} + Al^{3+}$ between dravite and elbaite in natural samples.

Surveys of the compositions of natural tourmalines by Foit and Rosenberg (1974, 1975, 1977) revealed the presence of additional coupled substitutions involving several structural sites. The most significant of these substitutions, which involve the schorl and dravite end-members are a dehydroxylation type, $(OH)^{-} + R^{2+} = O^{2-} + R^{3+}$ and an alkali-defect type, $R^{+} + R^{2+} = \square + R^{3+}$. These coupled substitutions produce intermediates between end-member schorl or dravite and a new series within the tourmaline group, $R^{+}_{1-x}R^{3+}_{3}Al_6(BO_3)_3Si_6O_{18}O_{3-x}(OH)_{1+x}$, which is defined by proton-deficient $[R^{+}R^{3+}_{3}Al_6(BO_3)_3Si_6O_{18}O_3(OH)]$ and alkali cation–free $[\square R^{3+}_{3}Al_6(BO_3)_3Si_6O_{18}O_2(OH)_2]$ end-members (Fig. 1). The loss of protons and alkali cations (principally Na) are charge-compensated by substitution of trivalent cations (R^{3+}) for divalent (R^{2+}) in principally the larger *9b* octahedral site (see Fig. 4 in Foit, 1989). The dashed line in Figure 1 shows the extent of these substitutions as determined by Foit and Rosenberg (1977). A study of a natural suite of tourmalines (Manning, 1982) has shown that substitution toward this series can occur within a single fractionation sequence.

0003–004X/89/1112–1317$02.00

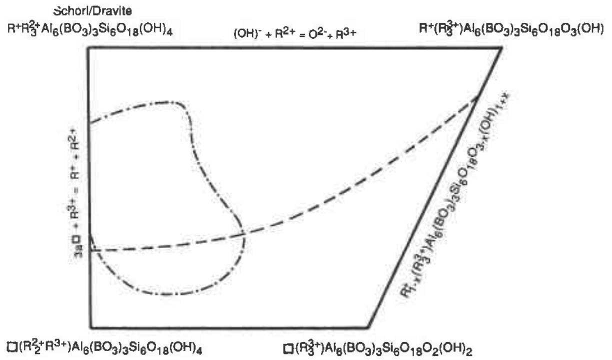

Fig. 1. Diagram showing the substitutional relationships between schorl or dravite and the hypothetical proton and alkali-cation deficient series, $R^{+}_{1-x}R^{3+}_{3}Al_6(BO_3)_3Si_6O_{18}O_{3-x}(OH)_{1+x}$, which is defined by proton-deficient $[R^{+}R^{3+}_{3}Al_6(BO_3)_3Si_6O_{18}O_3(OH)]$ and alkali cation–free $[\square R^{3+}_{3}R^{3+}_{6}(BO_3)_3Si_6O_{18}O_2(OH)_2]$ end-members. The dashed line shows the extent of substitution in natural samples reported by Foit and Rosenberg (1977), and the dot-dashed line gives the extent of substitution in the Jack Creek and Ben Lomond schorls.

Because the principal R^{3+} substituent is Al (Foit and Rosenberg, 1977), our investigations into the extent of these substitutions in nature has focused on deposits in which tourmalines coexist with Al-rich minerals. Preliminary examinations of the chemistry of schorls from tourmaline-dumortierite deposits at Jack Creek near Basin, Montana (Foit et al., 1989), and Ben Lomond, Hervey Range, North Queensland, Australia, have revealed tourmaline substitutional relationships more complex and structurally interesting than previously anticipated. The results of a more comprehensive study of the chemistry of tourmalines from these deposits are presented here.

LOCATION, GEOLOGY AND MINERALOGY OF THE TOURMALINE-DUMORTIERITE DEPOSITS

Jack Creek deposit

The Jack Creek dumortierite deposit (Fig. 2) is located on the west side of Jack Creek (NW¼, NE¼, sec. 14, T7N, R6W) in west-central Montana approximately 11 km northwest of the town of Basin.

The dominant rock types in the vicinity of the Jack Creek dumortierite deposit are welded tuffs of the Late Cretaceous Elkhorn Mountains volcanics and the slightly younger (~60 m.y.) quartz monzonites and subordinate granodiorites of the Boulder batholith (Ruppel, 1963), which intruded the tuffs at a shallow depth. The generally gradational batholith contact roughly follows Jack Creek and dips gently westward, attaining a depth of probably less than 500 m beneath the zone of dumortierite-tourmaline mineralization. This zone of mineralization in the altered roof rocks (metasomatized quartz latite welded tuffs) of the batholith is poorly exposed and largely seen only as blocks in a talus.

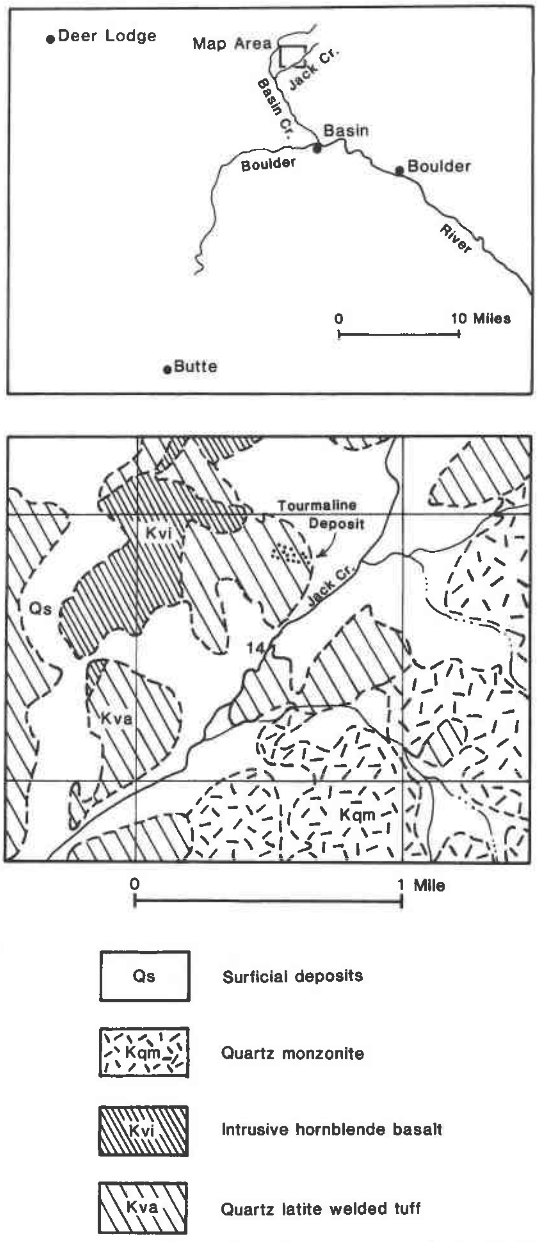

Fig. 2. Map showing the location and geology (by P. E. Myers) of the Jack Creek dumortierite deposit near Basin, Montana.

The host rock at the deposit is quartz latite welded tuff that has been metamorphosed to a fine-grained, light-colored rock containing quartz, plagioclase, alkali feldspar, sericite, chlorite, hematite, magnetite, limonite, dumortierite, and tourmaline (schorl). The dumortierite, $Al_7(BO_3)(SiO_4)_3O_3$, commonly occurs as fibrous, radiating aggregates 0.1–0.8 mm in diameter, as veinlets cutting across and along primary relict banding and as cavity fillings in tourmaline veins. The schorl, which seldom exceeds 10% of the rock except in very small areas, occurs as irregular fibrous patches and as cavity fillings in "dumortierized" rock and in dumortierite-poor veins cutting the altered tuff. Individual tourmaline crystals are typically subhedral and several tenths of a millimeter in maximum dimension. Tourmaline has also been reported in ore-bearing hydrothermal veins and pegmatites in the batholith rocks (Ruppel, 1963).

Ben Lomond deposit

The Ben Lomond uranium-molybdenum-zinc deposit is located in the Hervey Range, North Queensland, Australia, approximately 70 km west of Townsville. In the Ben Lomond area, a pile of calc-alkaline volcanic tuff ($\sim$1830 m thick) of late Paleozoic age lies unconformably on older Paleozoic strata and the crystalline basement. The volcanics are located in a half-graben structure and may be related to late activity of the Tasman Line subduction zone (Henderson, 1980; Oversby et al., 1980). The volcanics are divided into stratigraphically lower, Saint James, and upper, Cattle Creek, groups separated by an unconformity. Each of these units represents a series of volcanic cycles, each beginning with the venting of an andesite or basaltic andesite and ending with a silicic ignimbrite in response to a change from tensional to compressional tectonic conditions (Fuchs, unpublished manuscript). Both volcanic units appear to have undergone at least two stages of alteration. The first was alteration associated with cooling of the thick volcanic pile, and the second was the result of later convective hydrothermal activity associated with the shallow intrusion of the Pall Mall adamellite.

The later hydrothermal activity produced the tourmalinization and dumortierization that preceded uranium-molybdenum-zinc mineralization of the Ben Lomond deposit in the rhyolitic welded tuff at the top of the St. James volcanics (Valsardieu et al., 1980). The tourmalines examined in this study were collected by one of us (Y.F.) from altered rhyolites of Cattle Creek volcanics, the unit that appears to cap the hydrothermal system. Sample BL-215, collected in the vicinity of the Ben Lomond deposit, is from the central zone of the convective system, and sample BL-5 from Gympee, approximately 3.5 km to the southeast, is from the peripheral zone.

In both altered rhyolite samples, the glass is totally crystallized, and the matrix now largely consists of quartz with minor oxides and sulfides and massees of sericite, remnants of orthoclase phenocrysts. In addition, sample BL-215 from the central zone contains abundant andalusite and has total $SiO_2 + Al_2O_3$ values of >90 wt%. In sample BL-5 the tourmaline occurs with the sericite or iron oxides or more abundantly in centimeter-thick veins where early-formed quartz containing minor dumortierite is partially replaced by tourmaline. In BL-215 the tourmaline is found only in a vein where it grew perpendicularly to the wall. In a later stage of mineralization, the vein was filled with quartz and abundant violet dumortierite.

EXPERIMENTAL DETAILS AND DATA REDUCTION

Since the Jack Creek deposit is largely just a talus covered slope with very little outcrop, it was not possible to determine whether it is mineralogically zoned. Thus, the samples chosen (JC-1, JC-3, JC-4) for detailed analysis were those that exhibited the greatest macroscopic diversity. Polished coverless thin sections were prepared, and all sections contained in excess of 30% tourmaline, as irregular patches or as vein or vug fillings, and minor dumortierite. The tourmalines are strongly pleochroic with E = colorless to pale green and O = dark greenish blue. In basal sections the tourmaline was generally color zoned with pale green rims and dark blue or occasionally mottled or colorless cores. One hundred and eighty point analyses were systematically made on a total of 22 different crystals including basal and prismatic sections with a Cameca Cambax electron microprobe (Department of Geology, Washington State University) using wavelength-dispersive spectrometry, an accelerating voltage of 15 kV and a beam current of 7.7 nA. Ten elements (Ca, Na, Fe, Mg, Mn, Ti, K, Al, Si, and F) were present in measurable amounts; however, only the first nine were quantitatively determined.

Coverless, polished thin sections were made from Ben Lomond hand-samples BL-215 and BL-5. Tourmalines from both samples are strongly pleochroic with E = colorless to pale greenish yellow and O = greenish blue, and unlike the Jack Creek schorls, these are not appreciably zoned with respect to color or chemical composition. A total of 135 point analyses of approximately 90 crystals were made using the Cameca electron microprobes located in the Geology Departments of Washington State University and the Université Pierre et Marie Curie, Paris, France. In addition to those elements found in the Jack Creek schorls, the Ben Lomond schorls contain minor amounts of Ni, Zn, Cr, and U. Although never present in more than a few tenths of 1 wt%, they were nonetheless determined.

The coexistence of the Jack Creek tourmalines with hematite suggested the possibility that a significant portion of the Fe in these tourmalines was in the ferric state. Tourmaline concentrates from samples JC-3 and BL-5 (samples containing the most abundant and inclusion-free tourmaline) were prepared by heavy-liquid separation and hand picking. Analysis of the Mössbauer spectra of these concentrates yielded the site distributions of Fe^{2+} and Fe^{3+} given in Table 1.

The tourmaline formulas used in this study were calculated by assuming that B and (OH,F) are present in stoichiometric amounts. Cation site assignments were made by assuming that (1) Si deficiencies in the tetrahedral sites are compensated for by Al, (2) the smaller $18c$ octahedral site is occupied by Al and the proportions of Fe^{2+} given in Table 1, and (3) the remaining Mg, Mn, Fe^{2+}, Fe^{3+}, Al, and Ti cations occupy the larger $9b$ octahedral site. This generally resulted in a small $9b$ octahedral site vacancy and a significant $3a$ alkali-site vacancy. A bond-valence analysis of the Jack Creek tourmaline crystal used for the X-ray structural studies (Foit, 1989) suggests that these tourmalines are slightly OH deficient, which when taken into account reduces or eliminates the small octahedral defect.

TABLE 1. Fe^{2+}/Fe^{3+} distribution in Jack Creek and Ben Lomond schorls as determined from Mössbauer spectroscopy

	JC-3	BL-5
Fe^{3+} in 9*b* and 18*c* octahedral sites	18(3)	12(3)
Fe^{2+} in 9*b* octahedral site	50(3)	61(3)
Fe^{2+} in 18*c* octahedral site	32(3)	27(3)

Note: Numbers indicate percentage of total Fe with standard errors given in parentheses. Fe^{3+} contents of samples are too low to resolve contributions from 9*b* and 18*c* octahedral sites.

Tourmaline formulas calculated from analyses of sample BL-5 occasionally had excess Si (i.e., Si > 6 atoms per formula). Because electron-microscope examination revealed the presence of tiny (<1 μm) inclusions of quartz in some of the tourmaline crystals, these analyses were rejected. AEM analyses of the clean portions of included crystals generally had the same Al/Si ratios as electron-microprobe analyses of adjacent crystals that did not contain quartz inclusions.

TOURMALINE CHEMISTRY AND SUBSTITUTIONAL RELATIONSHIPS

Jack Creek schorls

The tourmalines are chemically zoned, aluminous schorls with relatively simple chemistries; the major cations present are Na, Fe, Mg, Al, and Si. The composition of the dark blue core and pale green rim of a typical zoned crystal is given in Table 2. The cores are richer in Fe and Al and poorer in Mg and Si than the rims. The compositional range for 97 point analyses of the cores of crystals is $(\square_{0.29-0.70}Na_{0.30-0.70}Ca_{0.00-0.06}K_{0.00-0.07})$ $(Fe^{2+}_{0.31-1.05}$ $Fe^{3+}_{0.11-0.38}$-$Al_{0.64-1.66}$ $Mg_{0.08-1.72}$ $\square_{0.00-0.29}$ $Ti_{0.00-0.15}$ $Mn_{0.00-0.03})$ $(Al_{5.33-5.80}$-$Fe^{2+}_{0.20-0.67})(BO_3)_3(Si_{5.43-5.99}Al_{0.01-0.57})O_{18}(OH,F)_4$ and that of 83 point analyses of the rims of the same crystals is $(\square_{0.20-0.88}Na_{0.11-0.76}Ca_{0.00-0.02}K_{0.00-0.04})(Fe^{2+}_{0.39-0.97}Fe^{3+}_{0.14-0.35}$-$Al_{0.63-1.60}Mg_{0.10-1.68}\square_{0.02-0.34}Ti_{0.00-0.03}Mn_{0.00-0.09})Al_{5.39-5.75}$-$Fe^{2+}_{0.25-0.61})(BO_3)_3(Si_{5.75-6.00}Al_{0.00-0.25})O_{18}(OH,F)_4$. The bulk of the compositional variability shown in Figures 3a and 3b is the product of alkali-defect and $^{[4]}Al$ (Tschermak's) substitutions:

$$R^+ + R^{2+} = {}^{3a}\square + R^{3+} \tag{1}$$

$$^{[4]}Al^{3+} + R^{3+} = Si^{4+} + R^{2+} \tag{2}$$

Equation 1 represents solid solution between schorl and a theoretical alkali-defect end-member $\square(R^{2+}_2R^{3+})Al_6(BO_3)_3Si_6O_{18}(OH)_4$. Equation 2 represents substitution of Al^{3+} for Si^{4+} in the six-membered tetrahedral ring with charge balance achieved by concomitant substitution of Al^{3+}, Fe^{3+}, and minor Ti^{4+} for divalent cations in the 9*b* octahedral site.

The alkali-defect substitution accounts for most of the compositional variability in the rims (Fig. 3b), whereas the Tschermak's substitution accounts for most of the variability observed in the cores (Fig. 3a). Furthermore, the trend of the data in Figure 3a suggests that significant substitution of Al for Si in the ring takes place in these tourmalines only when the 3*a* site is more than 40% occupied. The data in Figures 3a and 3b also show that the extent of these substitutions varies among samples; the alkali-defect substitution is more extensive in the JC-3 and JC-4 rims than in the JC-1 rims, whereas the Tschermak's substitution is more extensive in the JC-4 cores than it is in the JC-1 or JC-3 cores. This difference is also reflected in the covariance of the cation pairs R^+ and R^{3+} (9*b* + 18*c*) involved in the alkali-defect substitution, where $R^+ = Na^+ + K^+ + 2Ca^{2+}$ and $R^{3+} = Al^{3+} + Fe^{3+} + \frac{4}{3}Ti^{4+}$. R^+ is highly correlated to R^{3+} ($r = -0.90$), and the trend in this data (Fig. 4b) is parallel to that for the ideal defect-type substitution (line), whereas this ion pair

TABLE 2. Microprobe analyses and formulas of Jack Creek and Ben Lomond schorls

	Jack Creek (JC-4)*				Ben Lomond			
Oxide	Rim (wt%)	Cations	Core (wt%)	Cations	BL-5 (wt%)	Cations	BL-215 (wt%)	Cations
Na_2O	1.47(35)	0.46	1.73(11)	0.56	1.38(8)	0.44	0.84(11)	0.27
K_2O	0.02(1)	—	0.01(1)	—	0.01(1)	—	0.00	—
CaO	0.02(2)	—	0.01(2)	—	0.75(4)	0.13	0.12(3)	0.02
FeO	7.04(78)	0.96	9.73(88)	1.37	12.58(43)	1.76	9.79(21)	1.34
Fe_2O_3	1.71(11)	0.21	2.37(12)	0.30	1.91(6)	0.24	1.48(3)	0.18
MgO	3.46(65)	0.84	0.93(37)	0.23	0.62(19)	0.15	0.85(15)	0.21
MnO	0.00	—	0.01(1)	—	0.06(6)	0.01	0.06(3)	0.01
B_2O_3	10.70	3.00	10.30	3.00	10.42	3.00	10.60	3.00
Al_2O	35.23(71)	6.75	36.52(1.66)	7.26	35.24(50)	6.93	36.76(44)	7.11
TiO_2	0.06(4)	—	0.17(8)	0.02	0.20(5)	0.03	0.02(2)	—
SiO_2	36.97(74)	6.01	33.25(99)	5.61	34.23(41)	5.71	36.40(14)	5.98
H_2O	3.69	4.00	3.55	4.00	3.59	4.00	3.66	4.00
Total	100.38		98.58		100.99		100.58	
No. analyses	4		6		5		5	

Jack Creek rim: $(\square_{0.54}Na_{0.46})(Al_{1.12}Mg_{0.84}Fe^{2+}_{0.59}Fe^{3+}_{0.21}\square_{0.24})(Al_{5.63}Fe^{2+}_{0.37})(BO_3)_3Si_{6.01}O_{18}(OH)_4$

Jack Creek core: $(Na_{0.56}\square_{0.44})(Al_{1.41}Fe^{2+}_{0.83}Fe^{3+}_{0.30}Mg_{0.23}\square_{0.21}Ti_{0.02})(Al_{5.46}Fe^{2+}_{0.54})(BO_3)_3(Si_{5.61}Al_{0.39})O_{18}(OH)_4$

Ben Lomond BL-5: $(Na_{0.44}\square_{0.43}Ca_{0.13})(Fe^{2+}_{1.22}Fe^{3+}_{0.24}Al_{1.18}\square_{0.17}Mg_{0.15}Ti_{0.03}Mn_{0.01})(Al_{5.46}Fe^{2+}_{0.54})(BO_3)_3(Si_{5.71}Al_{0.29})O_{18}(OH)_4$

Ben Lomond BL-215: $(\square_{0.71}Na_{0.27}Ca_{0.02})(Al_{1.50}Fe^{2+}_{0.93}Fe^{3+}_{0.18}Mg_{0.21}\square_{0.15}Ti_{0.02}Mn_{0.01})(Al_{5.59}Fe^{2+}_{0.41})(BO_3)_3(Si_{5.98}Al_{0.02})O_{18}(OH)_4$

Note: Calculated assuming stoichiometric B and OH with cations normalized to 31(O,OH). Standard errors of the analyses given in parentheses.
* Core and rim of same crystal.

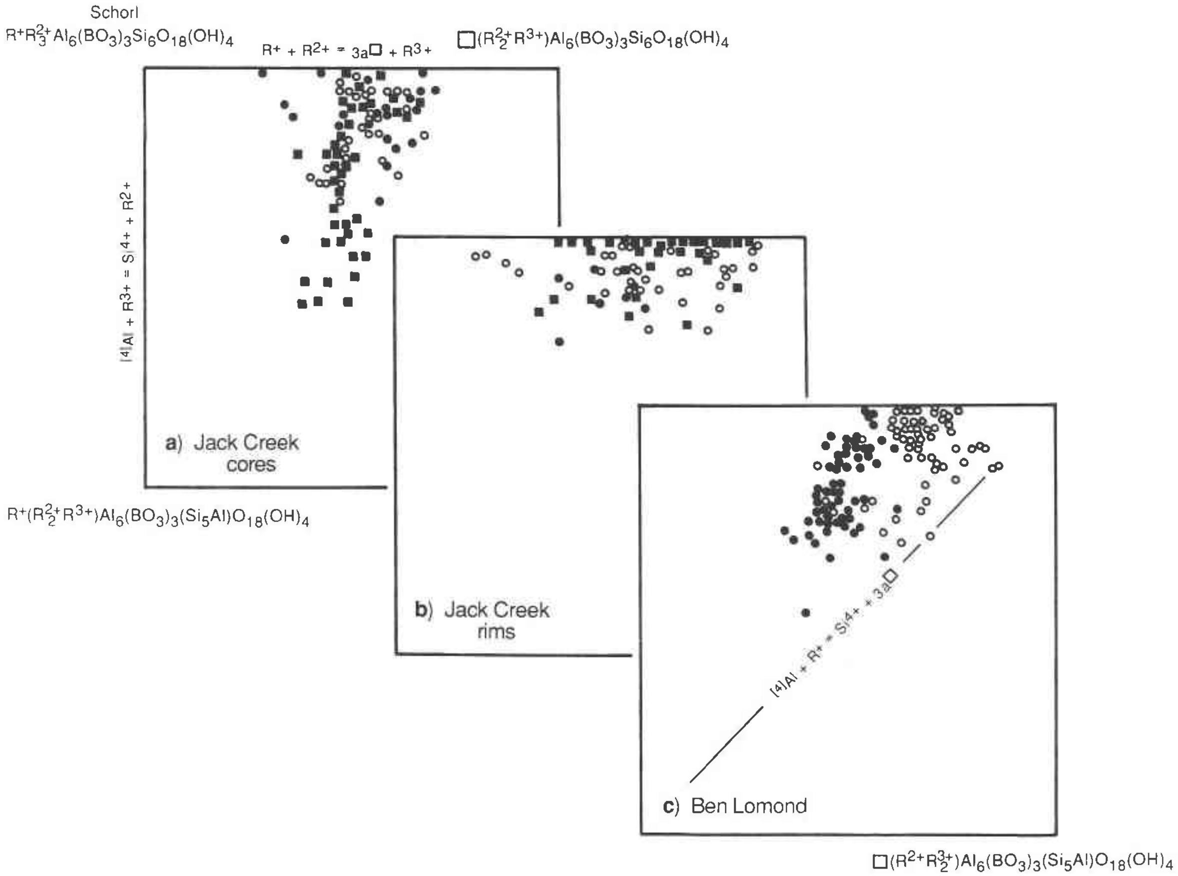

Fig. 3. Diagram showing tourmaline compositions. (**a**) Jack Creek schorl cores: filled circles, sample JC-1; open circles, JC-3; squares, JC-4. (**b**) Jack Creek schorl rims: filled circles, sample JC-1; open circles, JC-3; squares, JC-4. (**c**) Ben Lomond schorls: filled circles, sample BL-5; open circles, sample BL-215. Compositions plotted on the basis of alkali-site cation defect and [4]Al content.

is not significantly ($r = 0.02$) correlated in the cores (Fig. 4a). The most alkali-defective composition, $\square_{0.88}Na_{0.11}Ca_{0.01})(Al_{1.51}Fe^{2+}_{0.84}Fe^{3+}_{0.30}Mg_{0.14}\square_{0.20}Ti_{0.01})(Al_{5.46}Fe^{2+}_{0.54})(BO_3)_3(Si_{5.98}Al_{0.02})O_{18}(OH)_4$, which closely approximates that of the theoretical end-member, is from sample JC-3. In contrast, the extent of R^{3+} for R^{2+} substitution in the 9*b* site is highly correlated ($r = -0.73$) to the amount of Al^{3+} for Si^{4+} substitution in the tetrahedral ring of the cores (Fig. 5a) but not in that of the rims (Fig. 5b, $r = 0.08$). The tourmaline cores in sample JC-4 exhibit the widest range of $^{[4]}Al$ substitution with a maximum corresponding to composition $(Na_{0.54}\square_{0.42}K_{0.04})(Al_{1.64}Fe^{2+}_{0.68}Fe^{3+}_{0.24}\square_{0.24}Mg_{0.19}Ti_{0.01})(Al_{5.57}Fe^{2+}_{0.43})(BO_3)_3(Si_{5.44}Al_{0.56})O_{18}(OH)_4$. Although the Jack Creek schorls are not the most aluminous of tourmalines (e.g., elbaite is more aluminous), some are richer in $^{[4]}Al$ than any others so far described from nature.

The dehydroxylation substitution, $(OH)^- + R^{2+} = O^{2-} + R^{3+}$, which is so common in tourmalines (Foit and Rosenberg, 1977) is also present in the Jack Creek schorls. Although electron-microprobe analysis cannot directly provide information on the amount of H present in a sample, inferences regarding the extent of dehydroxylation in these tourmalines can be drawn from the bond-valence analysis of the structure of an alkali-deficient Jack Creek schorl (Foit, 1989). Calculation of bond valences assuming the Fe^{2+} and Fe^{3+} contents and distribution given in Table 1 and a stoichiometric amount of H (4 pfu) yields a significant oversaturation of O(1) and O(3), the two oxygens coordinated by protons, and a significant 9*b* octahedral vacancy (0.21 cations). Recalculation of the structural formula to provide O(1) and O(3) saturation reduces the (OH,F) stoichiometry to 3.38 pfu and completely eliminates the 9*b* site vacancy. If it is assumed that the presence of the small (averaging 0.16 cations or 5% of the site) but variable vacancy in the 9*b* octahedral site of the Jack Creek tourmalines is the result of dehydroxylation, the amount of dehydroxylation can be estimated by adjusting the OH stoichiometry to remove the vacancy. This procedure suggests that the average (OH,F) stoichiometry for the Jack Creek schorls is $(OH,F)_{3.52}$. Dehydroxylation, $(OH)^- + R^{2+} = O^{2-} + R^{3+}$, would also explain why the data in Figure 4b lie to the right of the trend of the alkali-defect substitution (i.e., are more R^{3+} rich).

Thus, the Jack Creek schorls are different from most

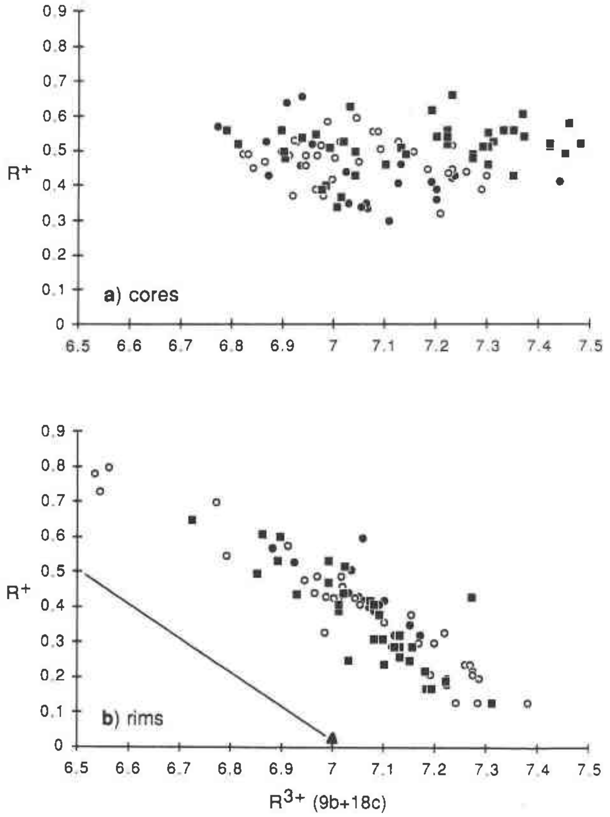

Fig. 4. Variation of R^+ with R^{3+} (9*b* + 18*c*). (**a**) 83 point analyses of the cores of 22 Jack Creek schorl crystals: filled circles, sample JC-1; open circles, JC-3; squares, JC-4. The line is the compositional trend of the alkali-defect substitution, $R^+ + R^{2+} = {}^{3a}\square + R^{3+}$, and the filled triangle represents the composition of end-member alkali-defect schorl, $\square(R^{2+}_2R^{3+})Al_6(BO_3)_3Si_6O_{18}(OH)_4$. (**b**) 97 point analyses of the rims of 22 Jack Creek schorl crystals: filled circles, sample JC-1; open circles, JC-3; squares, JC-4. Numbers of ions calculated on the basis of 31(O,OH).

tourmalines (Foit and Rosenberg, 1977) in that their compositional variability is dominated by the alkali-defect substitution and $^{[4]}Al$ substitution rather than by a dehydroxylation substitution (Fig. 1).

Ben Lomond schorls

Schorls in the two samples from the Ben Lomond deposit have generally different but overlapping chemistries (Table 2 and Fig. 3c). Tourmalines from the external zone (BL-5) are alkali-cation and $^{[4]}Al$ rich, having the compositional range $(\square_{0.35-0.62}Na_{0.28-0.60}Ca_{0.01-0.15}Mg_{0.00-0.01}K_{0.00-0.02})(Fe^{2+}_{0.96-1.48}Fe^{3+}_{0.19-0.29}Al_{0.79-1.41}Mg_{0.05-0.80}\square_{0.00-0.23}Mn_{0.00-0.12}Ti_{0.00-0.09}Cr_{0.00-0.02}Ni_{0.00-0.02})(Al_{5.35-5.57}Fe^{2+}_{0.43-0.65})(BO_3)_3(Si_{5.52-6.00}Al_{0.00-0.48})O_{18}(OH)_4$, whereas those from the internal zone (BL-215) tend to be more alkali-cation deficient and $^{[4]}Al$ poor, having the compositional range $(\square_{0.45-0.86}Na_{0.14-0.46}Ca_{0.00-0.13}K_{0.00-0.03})(Al_{1.16-1.75}Fe^{2+}_{0.46-1.37}Fe^{3+}_{0.09-0.27}Mg_{0.01-0.42}\square_{0.06-0.41}Ti_{0.00-0.05}Ni_{0.00-0.02}Zn_{0.00-0.02}Mn_{0.00-0.02}Cr_{0.00-0.01}U_{0.00-0.01})(Al_{5.39-5.79}Fe^{2+}_{0.21-0.61})(BO_3)_3(Si_{5.69-6.00}Al_{0.00-0.31})O_{18}(OH)_4$. BL-215 and BL-5 tourmalines are characterized not only by differences in the extent of the alkali-defect substitution as revealed by the clustering of data in Figure 3c but also by the apparent coupling of substitutions 1 and 2, especially in the BL-5 tourmalines. The compositional variability in the BL-5 tourmalines is best expressed by

$$^{[4]}Al^{3+} + R^+ = Si^{4+} + {}^{3a}\square, \qquad (3)$$

the substitution that relates the $^{[4]}Al$-substituted and alkali-defective compositions (Fig. 3c).

The BL-5 schorls generally contain more Ca than the BL-215 schorls (Fig. 6), and the Ca and $^{[4]}Al$ in the BL-5 schorls are positively correlated ($r = 0.74$), indicating that substitution of Al for Si in the ring is charge-compensated by the substitution of Ca in the nearly fully occupied 3*a* alkali-cation site. Therefore, for BL-5 tourmalines, substitution 3 is more appropriately written

$$2^{[4]}Al^{3+} + Ca^{2+} = 2Si^{4+} + {}^{3a}\square$$

or

$$^{[4]}Al^{3+} + Ca^{2+} = Si^{4+} + Na.$$

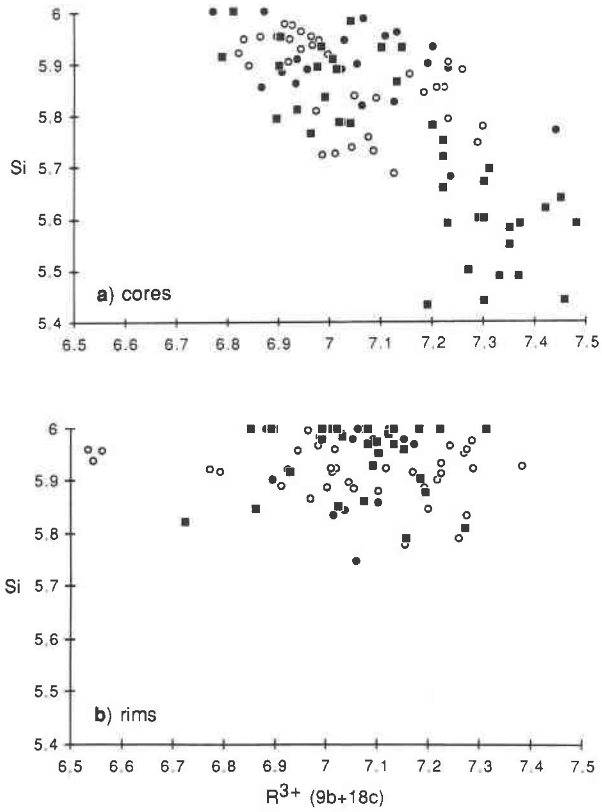

Fig. 5. Variation of Si with R^{3+} (9*b* + 18*c*). (**a**) 83 point analyses of the cores of 22 Jack Creek schorl crystals: filled circles, sample JC-1; open circles, JC-3; squares, JC-4. (**b**) 97 point analyses of the rims of 22 Jack Creek schorl crystals: filled circles, sample JC-1; open circles, JC-3; squares, JC-4. Numbers of ions calculated on the basis of 31(O,OH).

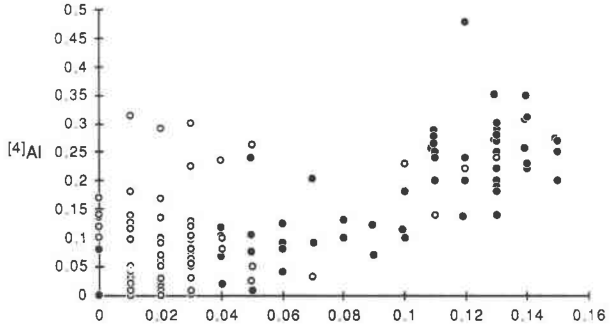

Fig. 6. Variation of $^{[4]}$Al with Ca for 135 point analyses of Ben Lomond schorl: filled circles, sample BL-5; open circles, sample BL-215. Numbers of ions calculated on the basis of 31(O,OH).

The alkali-defect substitution (Eq. 1), on the other hand, predominates in the BL-215 tourmalines (Fig. 7). This is verified by the high negative correlation (*r* = −0.69) between R^+ and R^{3+} (9*b* + 18*c*) observed for the BL-215 but not for the BL-5 tourmalines (*r* = −0.27). No significant covariance was observed between $^{[4]}$Al and R^{3+} (9*b* + 18*c*) (i.e., cations involved in the Tschermak's substitution) for either of the Ben Lomond tourmalines.

The average 9*b*-site vacancy is 0.14 cations for the BL-5 tourmalines and 0.21 for BL-215 tourmalines, suggesting a degree of dehydroxylation (OH,F) = 3.58–3.37 pfu, respectively, comparable to that observed for the Jack Creek schorls.

SUMMARY AND DISCUSSION

The compositional variations observed in schorls from two hydrothermally altered tuffs reflect the presence of the alkali-defect, $R^+ + R^{2+} = {}^{3a}\square + R^{3+}$, and $^{[4]}$Al substitutions. In the schorls from Jack Creek, substitution of Al for Si in the six-membered ring is charge-balanced by substitution of Al and, to a much less extent, Fe^{3+} for R^{2+} in the 9*b* octahedral site (Tschermak's substitution). In the schorls from the external zone (BL-5) $^{[4]}$Al substitution is primarily charge-compensated by either substitution of (Na,Ca) for a vacancy or Ca for Na in the 9-coordinated 3*a* alkali site. This accounts for the rather limited alkali-site defect found in tourmalines, especially those from Ben Lomond, which have the most extensive $^{[4]}$Al substitution. In addition, a small but variable amount of dehydroxylation, $(OH)^- + R^{2+} = O^{2-} + R^{3+}$, also takes place.

Similar cation substitutional relationships were observed in tourmalines synthesized in the system MgO-Al_2O_3-SiO_2-B_2O_3-H_2O over the temperature range 400–800 °C at a pressure of 1 kbar (Rosenberg and Foit, 1979, 1985). Like the Ben Lomond schorls (BL-215) from the interior and presumably higher-temperature zone, the tourmalines synthesized at higher temperatures have more 3*a* site defects and less $^{[4]}$Al substitution than those synthesized at lower temperatures. The synthesized tourmalines also show a positive correlation between the amounts of Mg in the 3*a* alkali site and Al in the tetrahedral site, analogous to the coupling between Ca and $^{[4]}$Al observed in the Ben Lomond schorls (BL-5) from the external zone. The tendency of Al for Si substitution to limit the amount of alkali-site defect (or vice versa) is due to the fact that 6 of the 9 oxygens coordinating the alkali-cation site are shared by only tetrahedral cations, principally Si. Therefore, substitution of Al in the tetrahedral ring creates valence undersaturation that can only be compensated by increased occupancy (increased valence saturation) of the 3*a* alkali site due to R^+ for □ or R^{2+} for R^+ substitutions. This explains (1) why the 3*a* alkali sites of synthetic and natural tourmalines with significant $^{[4]}$Al substitution usually contain divalent cations (Rosenberg and Foit, 1979, 1985; Rosenberg et al., 1986; Foit, 1989) and (2) the absence of natural tourmalines with compositions approaching $\square(R^{2+}R^{3+}_2)Al_6(BO_3)_3(Si_5Al)O_{18}(OH)_4$ (Fig. 3).

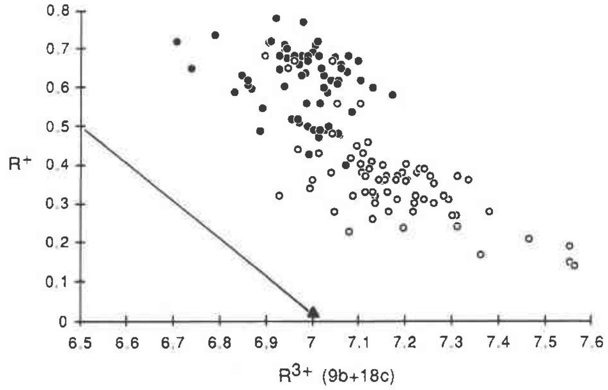

Fig. 7. Variation of R^+ with R^{3+} (9*b* + 18*c*) for 135 point analyses of Ben Lomond schorl: filled circles, sample BL-5; open circles, sample BL-215. The line is the compositional trend of the alkali-defect substitution, $R^+ + R^{2+} = {}^{3a}\square + R^{3+}$, and the filled triangle represents the composition of end-member alkali-defect schorl, $\square(R^{2+}_2R^{3+})Al_6(BO_3)_3Si_6O_{18}(OH)_4$. Numbers of ions calculated on the basis of 31(O,OH).

This study and several others (Rosenberg and Foit, 1979; Manning, 1982; Henry and Guidotti, 1985; Fuchs, 1987; Grew, 1988) show that tourmaline substitutional relationships are sensitive to the chemical and physical conditions that prevail during its crystallization. This sensitivity of tourmaline suggests that its careful chemical characterization during future petrologic studies may make it a useful petrogenetic indicator.

ACKNOWLEDGMENTS

We thank Prawit Towatana for help in collecting the data, M. Darby Dyer for collecting and interpreting the Mössbauer data, and Donald M. Burt for his critical review of the manuscript and his many helpful suggestions.

REFERENCES CITED

Foit, F.F., Jr. (1989) The crystal chemistry of alkali-deficient schorl and tourmaline structural relationships. American Mineralogist, 74, 422–431.

Foit, F.F., Jr., and Rosenberg, P.E. (1974) Coupled substitutions in tourmaline (abs.). EOS, 55, 467.

——— (1975) Aluminobuergerite, $Na_{1-x}Al_3Al_6B_3Si_6O_{27}O_{3-x}(OH)_{1+x}$, a new end-member of the tourmaline group (abs.). EOS, 56, 461.

——— (1977) Coupled substitutions in the tourmaline group. Contributions to Mineralogy and Petrology, 62, 109–127.

Foit, F.F., Jr., Towatana, P., and Myers, P.E. (1989) Alkali-deficient schorls from the Jack Creek tourmaline-dumortierite deposit, Jefferson County, Montana, Geological Society of America Abstracts with Programs, 21, 79.

Fuchs, Y. (1987) Zonalité des différents types de tourmaline dans le système hydrothermal de Novazza (Alpes Bergamasques, Italie du Nord). Comptes Rendus, l'Académie des Sciences, Paris, 305, Série II, 1507–1510.

Grew, E.S. (1988) Kornerupine at Sar-e-Sang, Afghanistan, white schist locality: Implications for tourmaline-kornerupine distribution in metamorphic rocks. American Mineralogist, 73, 345–357.

Henderson, R.A. (1980) Structural outline and summary geological history for northeastern Australia. In R.A. Henderson and P.J. Stephenson, Eds., The geology and geophysics of northeastern Australia, p. 1–26. Geological Society of Australia, Queensland Division, Brisbane, Australia.

Henry, D.J., and Guidotti, C.V. (1985) Tourmaline as a petrogenetic indicator mineral: An example from the staurolite-grade metapellite of NW Maine. American Mineralogist, 70, 1–15.

Manning, D.A.C. (1982) Chemical and morphological variation in tourmalines from the Hub Kapong batholith of peninsular Thailand. Mineralogical Magazine, 45(337), 139–147.

Oversby, B.S., Black, L.P., and Sheraton, J.W. (1980) Late Paleozoic continental volcanism in northeast Australia. In R.A. Henderson and P.J. Stephenson, Eds., The geology and geophysics of northeastern Australia, p. 247–268. Geological Society of Australia, Queensland Division, Brisbane, Australia.

Penfield, S.L., and Foote, H.W. (1899) XXIV. Ueber die chemische Zusammenstetzung des Turmalins. Zeitschrift für Kristallographie, 31, 321–352.

Riggs, R.B. (1888) The analysis and composition of tourmaline. American Journal of Science, 35, 35–51.

Rosenberg, P.E., and Foit, F.F., Jr. (1979) Synthesis and characterization of alkali-free tourmaline. American Mineralogist, 64, 180–186.

——— (1985) Tourmaline solid solutions in the system MgO-Al_2O_3-SiO_2-B_2O_3-H_2O. American Mineralogist, 70, 1217–1223.

Rosenberg, P.E., Foit, F.F., Jr., and Ekambaram, V. (1986) Synthesis and characterization of tourmaline in the system Na_2O-Al_2O_3-SiO_2-B_2O_3-H_2O. American Mineralogist, 71, 971–976.

Ruppel, E.T. (1963) Geology of the Basin quadrangle, Jefferson, Lewis and Clark, and Powell Counties, Montana. U.S. Geological Survey Bulletin 1151, 121 p.

Valsardieu, C.A., Cocquio, D.S., and Bauchau, C. (1980) Uranium-molybdenum mineralization at Ben Lomond, Hervey Range, North Queensland, Australia. Proceedings of the Australian Institute of Mining and Metallurgy, 273, 27–35.

MANUSCRIPT RECEIVED SEPTEMBER 6, 1988
MANUSCRIPT ACCEPTED JULY 26, 1989